論文 / 著書情報
Article / Book Information

Title	Damage Evaluation of Full-Scale Steel Gymnasium based on E-Defense Shaking Table Tests
Authors	Daiki SATO, Rie SUZUKI, Hotsuki WADA, Tomohiro SASAKI, Atsushi AOI, Hiroyuki TAGAWA, Koichi KAJIWARA
Conference	7th Structural Engineers World Congress 2019
Citation	This article is taken from the Proceedings of SEWC ’ 19 International Structural Engineers World Congress on Architecture and Structure: from Past to Future, pp. 1009-1020, April 2019, Istanbul Turkey, ISBN:978-605-62703-8-3

DAMAGE EVALUATION OF FULL-SCALE STEEL GYMNASIUM BASED ON E-DEFENSE SHAKING TABLE TESTS

Daiki Sato[1], Rie Suzuki[2], Hotsuki Wada[3], Tomohiro Sasaki[4], Atsushi Aoi[2], Hiroyuki Tagawa[5] , Koichi Kajiwara[6]

[1] Tokyo Institute of Technology

[2] Takenaka Corporation

[3] Tomoe Corporation

[4] Obayashi Corporation

[5] Mukogawa Women's University

[6] National Research Institute for Earth Science and Disaster Resilience

Keywords: Full-Scale Gymnasium, E-Defense, Natural Frequency, Damping Ratio, Mode Shape

Abstract

During the 2011 Tohoku earthquake off the Pacific coast of Japan, destruction of the column base and brace of a school gymnasium, which is a large spacious building, was reported. In addition, many cases of ceiling material and equipment falling were also reported. The school gymnasium is an evacuation base for local residents during the occurrence of large earthquakes. Considering its function and the importance of protecting life, such damage is unacceptable. To prevent the falling of a ceiling, many studies on the mechanisms leading to the fall of the ceiling and evaluation of the associated stress have been carried out.

Large earthquakes cause damage to the frame and brace of a building. It is necessary to study the change in vibration characteristics of the roof caused by plasticization. Therefore, the aim of this study is to evaluate the damage caused in a full-scale steel gymnasium based on E-Defense shaking table tests.

An analysis of the natural frequency of the specimen by plasticization is also performed. Next, focusing on the fall of the wall brace, roof brace, and ceiling of the test structure, the relationship between the scope of damage and change of the natural frequency is analyzed. In addition, by analyzing an accelerometer installed on the roof surface, the response of the steel gymnasium during a large earthquake is examined. Lastly, changes in the damping ratio and mode shape of the specimen are studied using the frequency domain decomposition (FDD) method.

1 INTRODUCTION

During the 2011 Tohoku earthquake off the Pacific coast of Japan, destruction of the column base and brace of a school gymnasium, which is a large spacious building, was reported. In addition, many cases of ceiling material and equipment falling were also reported. The school gymnasium is an evacuation base for local residents during the occurrence of large earthquakes. Considering its function and the importance of protecting life, such damage is unacceptable. To prevent the falling of a ceiling, many studies on the mechanisms leading to the fall of the ceiling and evaluation of the associated stress have been carried out. Some of the damage to the ceiling caused by the 2011 Tohoku earthquake is thought to have amplified the response of the suspended ceiling due to resonance with the structural frame. Therefore, it is necessary to analyze not only the ceiling, but also the response of the roof surface in detail. In the current ceiling seismic design, we assume a rigid ceiling supported by a rigid roof. However, when the plastic deformation or buckling in the braces is induced by the earthquake, the stiffness of the gymnasium using the brace structure decreases. Therefore, the rigid floor assumption is not applicable. In addition, the range of external forces for the ceiling design is based on medium earthquakes; hence, large earthquakes are not covered. However, because the fall of the ceiling involves safety, it is necessary to consider the external force of large earthquake motion, where plasticity occurs in the structural frame, for the ceiling design. Many experimental studies based on the falling of ceilings are vibration experiments performed by hanging the ceiling under a rigid frame structure. Therefore, further research is required to study the influence of complicated behavior particular to the space structure on the ceiling.

Large earthquakes cause damage to the frame and brace of a building. It is necessary to study the change in vibration characteristics of the roof caused by plasticization. Therefore, the aim of this study is to evaluate the damage caused in a full-scale steel gymnasium based on E-Defense shaking table tests. An analysis of the natural frequency of the specimen by plasticization is also performed. Next, focusing on the fall of the wall brace, roof brace, and ceiling of the specimen, the relationship between the scope of damage and change of the natu-ral frequency is analyzed. In addition, by analyzing an accelerometer installed on the roof sur-face, the response of the steel gymnasium during a large earthquake is examined. Lastly, changes in the damping ratio and mode shape of the specimen are studied using the frequency domain decomposition (FDD) method [3].

2 OUTLINE OF EXPERIMENT

2.1 Outline of specimen

Figure 1 shows a photograph of the entire specimen, and Table 1 shows the main specifications of the specimen. The test structure is a steel frame gymnasium with a ceiling-shaped roof and is designed for use as a gymnasium at elementary and junior high schools. The plane dimension of the specimen is 18.6 m × 30 m. The roof gradient is set to 10:3 so that the rise span ratio becomes 0.15, and the test structure height is 9.09 m at the tallest point. A suspended ceiling having the same gradient as the roof surface is installed in the test structure. We changed the ceiling during the experiment and carried out the experiment twice. One ceiling test specimen is an unmeasured ceiling without countermeasures against earthquakes, and the other is an earthquake-resistant ceiling on which fall-prevention measures were applied. In this paper, the test specimen with the unmeasured ceiling is called "non-seismically designed ceiling specimen" (NC-specimen) and the specimen with earthquake resistant ceiling is called "seismically designed ceiling specimen" (SC-specimen). The details of the test specimens are described in References [1, 2].

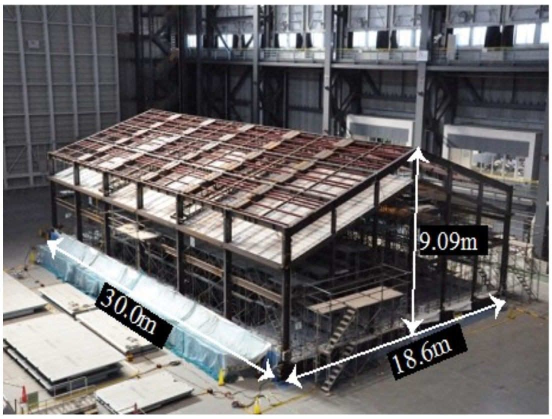

Figure 1: Full-scale gymnasium specimen

Table 1: Specification of gymnasium specimen

Item		Specification
Structure		One-story steel gymnasium
Mass	Superstructure	71t (Without weight on roof)
	Weight on roof	30 t
	Total	230 t
Height		9.090 m
Plan Size		30.0 m×18.6 m (6 spans×6 spans)
Design		Allowable stress design (Base-shear coefficient $C_0 = 0.2$)
Members	Column	H400×200×8×13 (SS400)
		H250×125×6×9 (SS400) H300×150×6.5×9 (SS400)
	Girder	H400×200×8×13 (SS400)
	Beam	H248×124×5×8 (SS400)
	Wall Braces	M20, M27 (SNR400B) Pipe-type Turnbuckle
	Roof Braces	M16 (SNR400B) Pipe-type Turnbuckle

2.2 Excitation plan

Acceleration records observed in Sendai during the 2011 Tohoku earthquake (K-NET Sendai) and in Kobe Maritime Atmosphere during the 1995 Kobe earthquake (JMA Kobe wave) were used. In both K-NET Sendai and JMA Kobe, the NS component was input into the span direction (Y-direction), EW component was input into the ridge direction (X-direction) and UD component was input into the vertical direction (Z-direction), respectively. The acceleration time histories of the K-NET Sendai and JMA Kobe are shown in Figure 2, and the acceleration response spectrum (Damping ratio h = 5%) is shown in Figure 3. As a reference, spectra of the Extremely-Rare level indicated by the Building Standards Law of Japan (BSLJ) are also included in Figure 3. In the experiment of NC-specimen, 50% excita-tion was induced twice, and then K-NET Sendai was modeled with 5% and 25% excitation (hereafter denoted by K-NET Sendai 5% and 25%, for example). In the experiment of SC-specimen, after K-NET Sendai was induced with 5%, 25%, 50%, 80%, and 100% excitation, JMA Kobe was induced with 100% and 150% excitation. Table 2 shows the outline of the in-put level of the excitation wave and excitation exercise number. To understand the frequency of the specimen before and after each excitation, random wave excitation is analyzed.

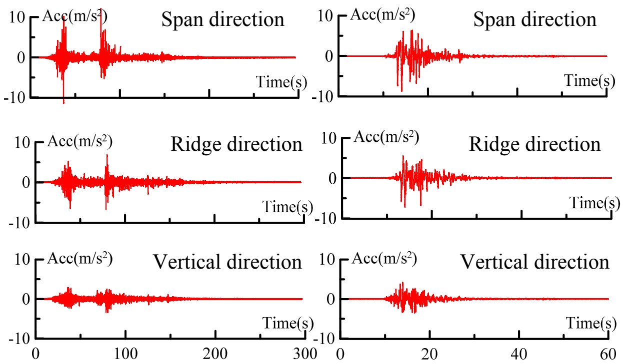

(a) K-NET Sendai 100% (b) JMA Kobe 100%

Figure 2: Input acceleration time histories

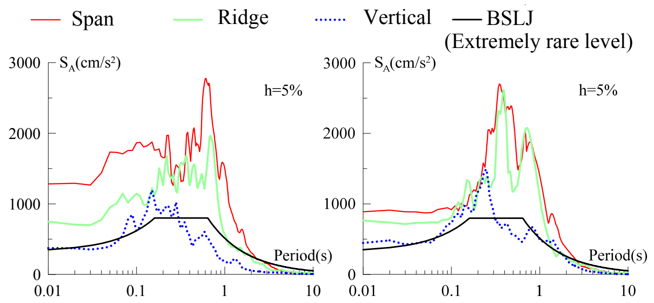

(a) K-NET Sendai 100% (b) JMA Kobe 100%

Figure 3: Acceleration response spectrum

Table 2: Input level of the excitation wave and excitation number (No.)

Day	2014/1/27									2014/1/28						
Specimen	Non-seismically designed ceiling specimen (NC-specimen)															
No.	2	3	4	5	6	7	8	9	10	11	12	13	14	15	16	17
Name	Random (Span)	Random (Ridge)	Random (Vertical)	Random (3 axis)	K-NET Sendai 3%	K-NET Sendai 5%	Random (3 axis)	JMA-Kobe 5%	Random (3 axis)	Random (3 axis)	K-NET Sendai 25%	Random (3 axis)	K-NET Sendai 50%	Random (3 axis)	K-NET Sendai 50%	Random (3 axis)

Day	2014/2/27											2014/2/28								
Specimen	Seismically designed ceiling specimen (SC-specimen)																			
No.	18	19	20	21	22	23	24	25	26	27	28	29	30	31	32	33	34	35	36	37
Name	Random (Span)	Random (Ridge)	Random (Vertical)	Random (3 axis)	K-NET Sendai 5%	Random (3 axis)	K-NET Sendai 25%	Random (3 axis)	Random (3 axis)	K-NET Sendai 50%	Random (3 axis)	Random (3 axis)	K-NET Sendai 80%	Random (3 axis)	K-NET Sendai 100%	Random (3 axis)	JMA-Kobe 100%	Random (3 axis)	JMA-Kobe 100%	Random (3 axis)

2.3 Measurement plan

The locations of the accelerometers and strain gauges are shown in Figures 4, 5, and 6. Acceleration and strain are measured in 0.001 s time intervals. The details of the measurement plan and its accuracy are described in Reference [1, 2, 4].

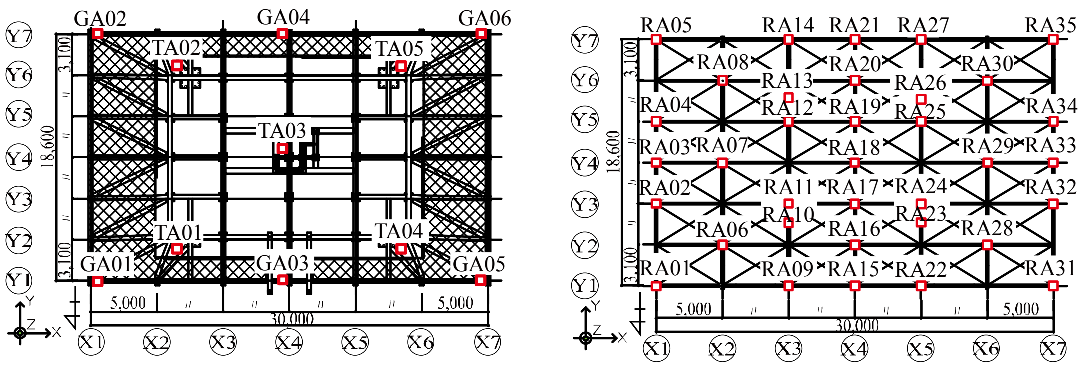

(a) Shaking table and column base (b) Roof

Figure 4: Location of accelerometer (unit: mm)

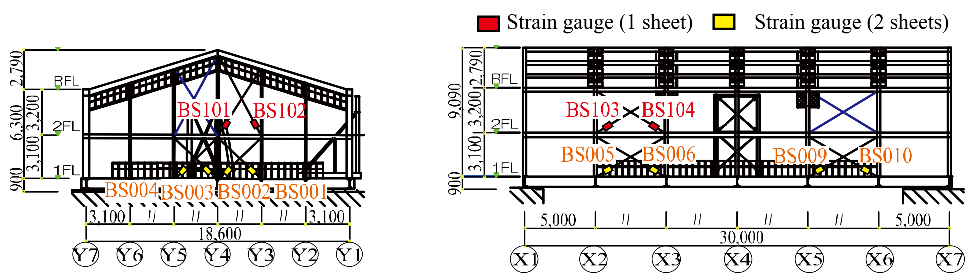

(a) Elevation X1 (b) Elevation Y1

Figure 5: Location of strain gauge of wall brace (unit: mm)

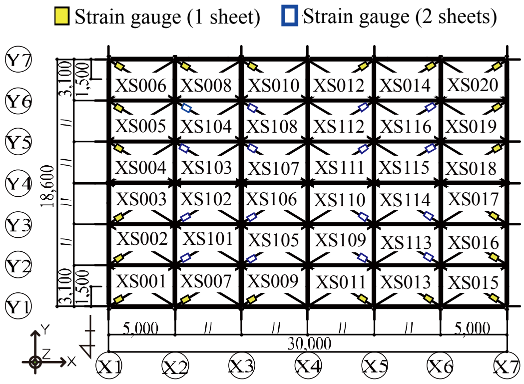

Figure 6: Location of strain gauge of roof brace (unit: mm)

3 ANALYSIS OF CHANGES IN FIRST NATURAL FREQUENCY

3.1 Analysis method and results

In each random wave excitation, a transfer function (input: shaking table, output: roof, RA19; see Figure 4 (b)) is calculated, and the first peak is estimated as the first natural frequency [5]. Figures 7(a) and (b) illustrate the transfer function of NC-specimen and SC-specimen on the RA19 in the ridge direction, respectively. Both figures show the results of the first excitation (solid line) and last excitation (broken line), respectively. From Figures 7(a) and (b), it can be confirmed that the peak of the first natural frequency can be observed. It is also found that the value of the peak of the transfer function is lower in the last random wave excitation (broken line) than in the first random wave excitation (solid line).

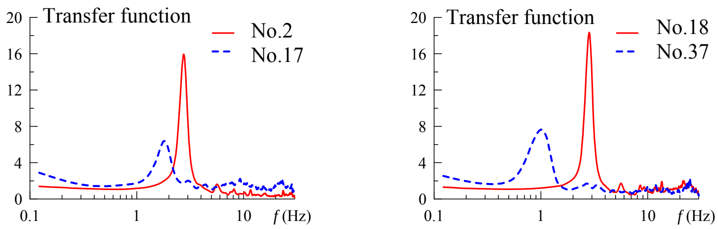

(a) NC-specimen (b) SC-specimen

Figure 7: Transfer function (RA19, Ridge direction)

3.2 Changes in natural frequency

Figure 8 shows the change in the first natural frequency of each random wave estimated from the transfer function. The horizontal axis shows the excitation exercise number (Table 2), and the vertical axis shows the first natural frequency in each direction. In NC-specimen, the ceiling fell during K-NET Sendai 50% (No. 17) excitation. On the other hand, in SC-specimen, the ceiling fell during K-NET Sendai 100% (No. 34) and JMA Kobe 150% (No. 36) excitations. The conditions of the fall of the ceiling are shown in Figures 9(a) and (b), respec-tively. The mechanism of the fall of the ceiling is described in detail in Reference [1]. From Figure 8, it can be seen that after No. 17, the natural frequency increases significantly. This is because the brace was re-tightened when the ceilings were changed. From this, it is believed that the stiffness changes due to the loosening of the brace cause the natural frequency to also change. In addition, it can be seen from Figure 8 that the first natural frequency decreases as the input level increases, and the change varies with the direction. This trend was also con-firmed in places other than RA 19.

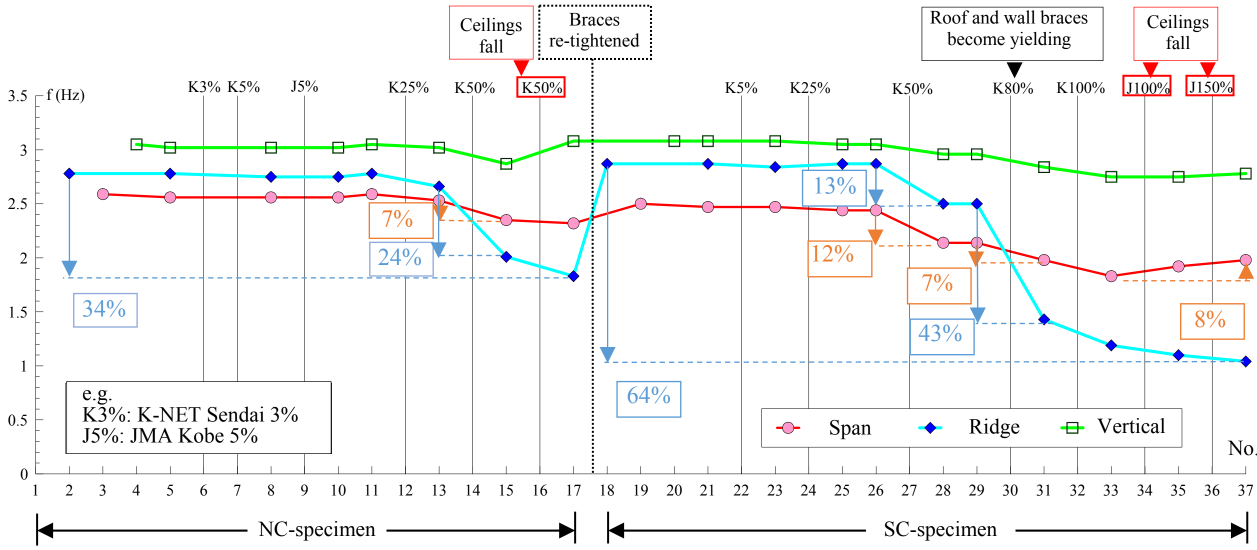

Figure 8: Changes in first natural frequency in each direction (RA19)

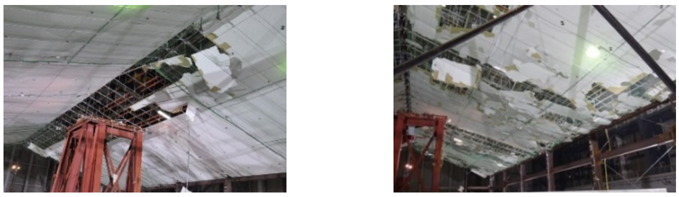

(a) NC-specimen (After No. 17) (b) SC-specimen (After No. 37)

Figure 9: Conditions of the ceiling fall

4 DAMAGE OF THE TEST SPECIMEN

4.1 Damage of wall brace

The plasticity of the wall brace is evaluated from the strain time history data. When K-NET Sendai 25%, 50%, 80%, and 100% (No. 24, 27, 30, 32) are input to SC-specimen, the time histories of the wall brace strain (BS005; Figure 5(b)) are shown in Figures 10(a)–(d), respectively. From Figure 10, it can be confirmed that additional tensile strain appears without strain showing negative compression. The brace is elastic when the input level is 50% or less. However, the tensile yield occurs in the brace when the input level is 80% or more. Figure 11 shows the percentage of wall braces where tensile yielding occurred. From Figure 11, it can be confirmed that the wall braces do not experience tensile yield ($\varepsilon < \varepsilon_y$) until K-NET Sendai 50% (No. 27). However, many wall braces experience tensile yield ($\varepsilon > \varepsilon_y$) on both the X1 and X7 side and the Y1 and Y7 side in the case of the K-NET Sendai 80% (No. 30). Figure 12 illustrates the tensile yielding order of the wall brace at K-NET Sendai 80% (No. 30) in SC-specimen. At the beginning, the wall braces on Y1 and Y7 side reach tensile yield, but after that the tensile yield occurs in all wall braces on the X1 and X7 side, and then wall braces on the Y1 and Y7 side reach tensile strain.

Figure 13 shows a photograph of the wall brace of NC-specimen after completion of No. 17 excitation. It was confirmed that the wall brace was slightly curved out of plane by both photograph and observation after the experiment. In the time history of the strain gauge, it is confirmed that the strain of the wall brace does not reach the tensile yield strain. However, as shown in Figure 8, during the change in natural frequency, it is possible that the wall brace was compression buckling when NC-specimen was excited with K-NET Sendai 50% (No. 16).

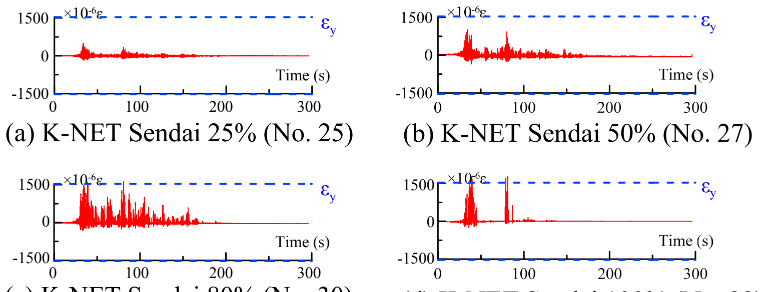

(a) K-NET Sendai 25% (No. 25) (b) K-NET Sendai 50% (No. 27)

(c) K-NET Sendai 80% (No. 30) (d) K-NET Sendai 100% (No. 32)

Figure 10: Time histories of wall brace strain (BS005, SC-specimen)

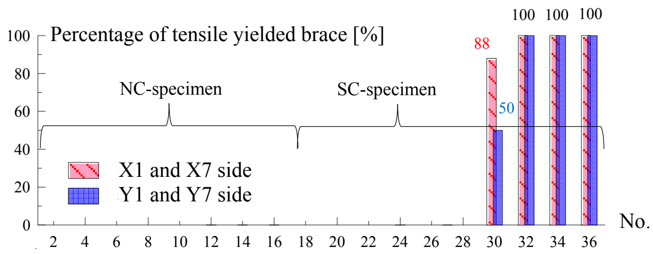

Figure 11: Percentage of tensile yielded wall brace [%]

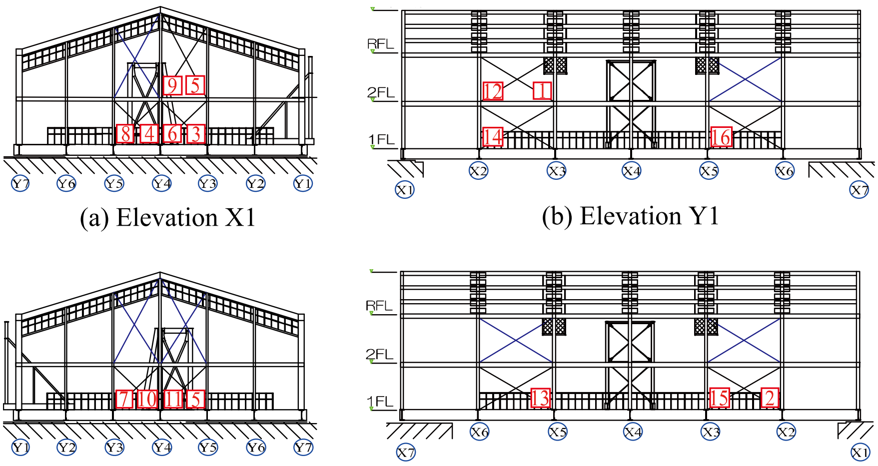

(a) Elevation X1 (b) Elevation Y1

(c) Elevation X7 (d) Elevation Y7

Figure 12: Tensile yielding order of wall brace (SC-specimen)

Figure 13: Photograph of wall brace of NC-specimen after No. 17 excitation (Y1 and Y7 side)

4.2 Damage of roof brace

The time histories of the roof brace (XS101; Figure 6) strain are shown in Figure 14 when K-NET Sendai 25%, 50%, 80%, and 100% (No. 24, 27, 30, 32) are input to SC-specimen. From Figure 14, it is confirmed that the roof brace does not reach tensile strain ε_y when the input level is 50% or less. However, tensile yield occurs in the brace when the input level is 80% or more. Figure 15 shows the percentage of wall braces where tensile yielding occurred. It is confirmed that all the roof braces do not experience tensile yield up to K-NET Sendai 50% (No. 27) in SC-specimen. However, in the case of K-NET Sendai 80% (No. 30), 69% of the roof braces reach tensile strain. In addition, tensile yield has occurred in all roof braces when JMA Kobe 100% is input (No. 34). Therefore, it is believed that the stiffness of the roof surface is degraded. Figure 16 illustrates the tensile yielding order obtained from the time history of the roof brace strain. From Figure 16, it can be seen that tensile yield has occurred in many roof braces when K-NET Sendai 80% (No. 30) is input into SC-specimen. First, the roof brace at the outer peripheral part reaches tensile strain quickly. Then the brace which is next to it or near it becomes tensile yielding. At K-NET Sendai 100% (No. 32), tensile yielding also occurs in the inside roof braces.

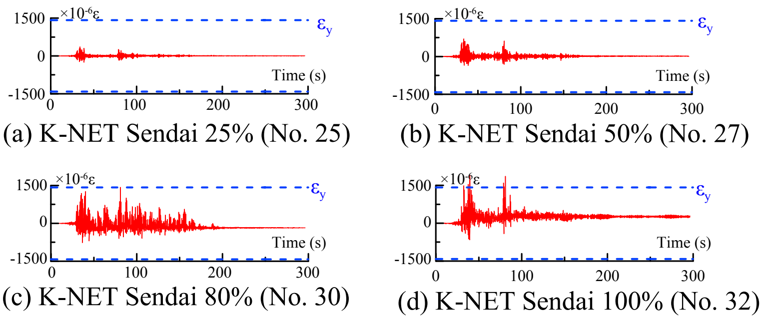

(a) K-NET Sendai 25% (No. 25) (b) K-NET Sendai 50% (No. 27)

(c) K-NET Sendai 80% (No. 30) (d) K-NET Sendai 100% (No. 32)

Figure 14: Time histories of roof brace strain (XS101, SC-specimen)

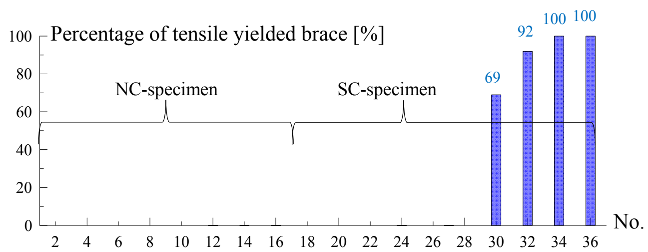

Figure 15: Percentage of tensile yielded roof brace [%]

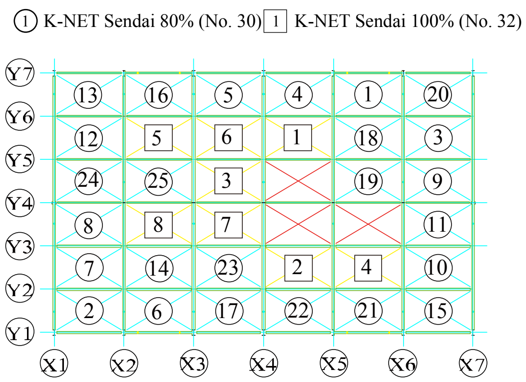

Figure 16: Tensile yielding order of roof brace (SC-specimen)

5 CHANGE IN DAMPING RATIO AND MODE SHAPE

5.1 Change in damping ratio

Damping ratio of the test specimen is obtained by the FDD method [3]. A band pass filter of 0.9 to 1.1 times the peak frequency of the singular value curve is applied [6], and the autocorrelation function is calculated by inverse Fourier transformation. The autocorrelation function is applied to the theoretical curve of free vibration, and the damping constant is estimated. Figure 17 shows the autocorrelation function (solid line) obtained by FDD method and the theoretical curve of free vibration (broken line). From Figure 17, it is understood that the theoretical curves of free vibration in the span and ridge directions agree well with the autocorrelation function. Even if the specimen were damaged, it was possible to perform the identification with high accuracy. The estimated damping ratios are shown in Figure 18. From Figure 18, it can be confirmed that the damping ratio in the span direction rises after K-NET Sendai 50%, where the decrease of natural frequency is confirmed. The damping ratio in the ridge direction was confirmed to rise after K-NET Sendai 50% (No. 27), and the damping ratio increased after K-NET Sendai 80% (No. 30), where the natural frequency was greatly reduced. Much like the natural frequency shown in Figure 8, the damping ratio of the vertical direction slightly changes.

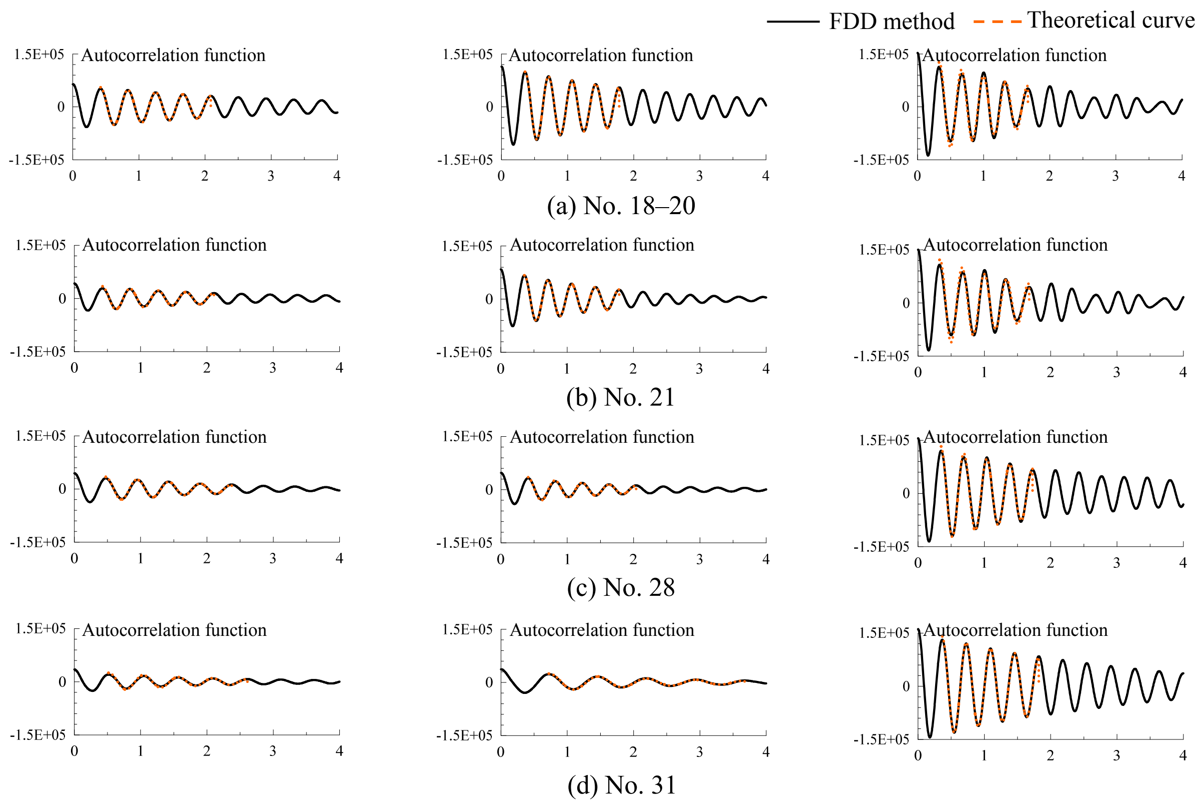

Figure 17: Autocorrelation function (From rest side: span, ridge, and vertical directions)

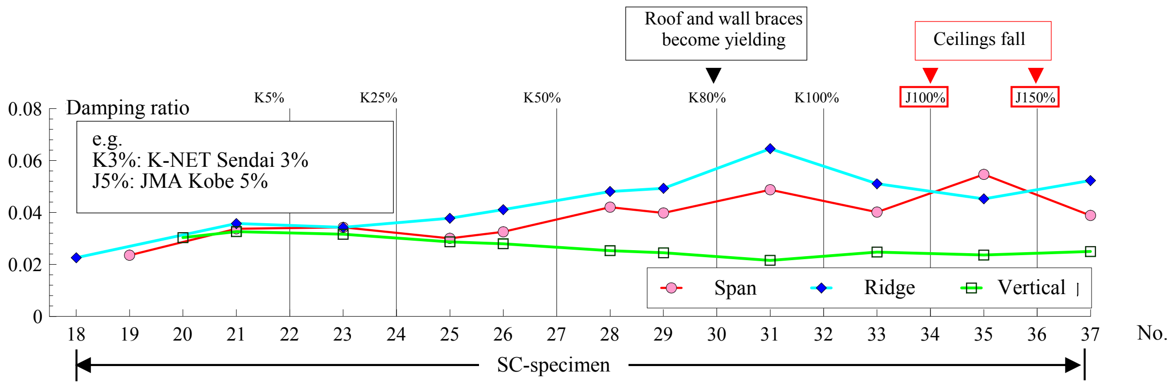

Figure 18: Identification results of first damping ratio of SC-specimen

5.2 Change in first mode shape

The first mode shape is identified from the singular value vector. First, by using the experimental results with no damage (No. 21), the identification accuracy of the FDD method of mode shape is verified. The mode shape is standardized in each direction using the RA 18 located at the center of the specimen (Figure 4(b)). The identified first mode shapes in each direction are shown in Figures 19(a)–(d), respectively. From Figure 19, it was confirmed that the identification result by the FDD method roughly agrees with the mode shape of the eigenvalue analysis result of the analytical model that was performed in advance.

Next, comparisons of the mode shapes identified from the experimental results before (solid line, No. 21) and after damage (broken line, No. 37), in each direction, are shown in Figure 20, respectively. The acceleration data points at the position where the accelerometer is not installed were found by linear interpolation using the peripheral acceleration data points. The tensile yield occurred on the wall and roof braces, and the first natural frequency decreased by 19% on the span direction and 64% on the ridge direction (Figure 8). However, as shown in Figure 20, it can be confirmed that the first mode shape in each direction does not change significantly.

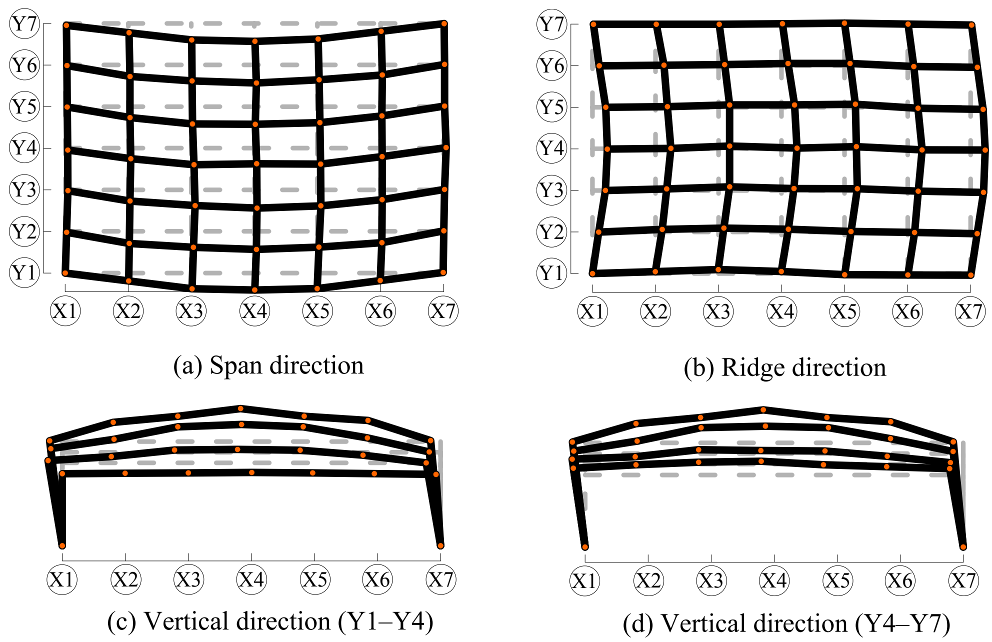

Figure 19: Identified first mode shapes in each direction (No. 21, SC-specimen)

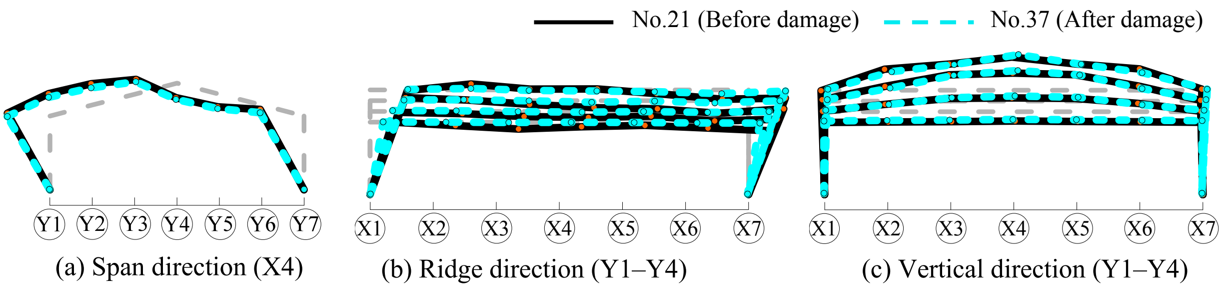

Figure 20: Comparison of identified first mode shapes in each direction (SC-specimen)

6 CONCLUSIONS

In this study, we analyzed the change in natural frequency resulting from the decrease in rigidity due to the damage of material in continuous excitation. Experiments were performed on a full-scale steel gymnasium test structure using E-Defense. In addition, the relationship between the scope of the damage to the wall and roof brace of the specimen and change in the first natural frequency was evaluated. Changes in the first damping ratio and mode shape of the specimen were also studied using the FDD method.

ACKNOWLEDGEMENTS

The shake table experiment on full-scale school gymnasium specimen with wide-area suspended ceiling was conducted based on the extensive support of Large-space School Structure’s Experimental Research Committee (Chief Professor Toshimi Kabeyasawa (The Tokyo University), Associate Professor Tsuyoshi Seike(The Tokyo University), Professor Satoshi Yamada (Tokyo Institute of Technology), Dr. Hiroshi Fukuyama (National Research Institute for Land and Infrastructure Management)) and Experimental Planning Working Group (Chief Dr. Tomohiro Sasaki (National Research Institute for Earth Science and Disaster Resilience), Mr. Tsutomu Ota (Horie Engineering and Architectural Research Institute Co., Ltd), Associate Professor Toru Eguchi (Yokohama National University), Associate Professor Jun Iyama (The University of Tokyo), Dr. Tadashi Ishihara (Building Research Institute))for experimental plan and design of steel gymnasium specimen and suspended ceilings. The authors greatly appreciated to give important information about damage of school and cultural facilities in recent earthquake by Mr. Mitsugu Hirota (MEXT, Ministry of Education, Culture, Sports, Science and Technology). The autors also greatly appreciated to be advised about experimental plan by Committee for Advance of Seismic Countermeasures for Nonstructural Components in School Facilities held by MEXT.

REFERENCES

[1] Tomohiro SASAKI, Atsushi AOI, Koichi KAJIWARA, Hiroyuki TAGAWA and Daiki SATO. 2017. “Collapse Mechanism of Wide-area Suspended Ceiling Based on Full-Scale Shake Table Experiment of School Gymnasium”. *Proceedings of the 16th World Conference on Earthquake Engineering*, 2935.

[2] Tomohiro SASAKI, Atsushi AOI, Hiroyuki TAGAWA, Koichi KAJIWARA, Daiki SATO, Toshimi KABEYASAWA, Tsuyoshi SEIKE, Satoshi YAMADA Hiroshi FUKUKYAMA. 2017. “Design and Structural Response of Full-Scale Steel Gymnasium

Specimen. E-Defense shake table experiment on collapse mechanism of wide-area suspended ceiling in gymnasium part 1". *Journal of Structural and Construction Engineering (Transactions of AIJ).* AIJ, LVol.82 No.736, Pp:831-841. (in Japanese)

[3] Brincker, R.，L. Zhang，P. Andersen. 2000. "Modal Identification from Ambient Responses Using Frequency Domain Decomposition". *Proc. of 18th International Modal Analysis Conference*, Pp:625-630.

[4] Tomohiro SASAKI, Daiki SATO, Rie SUZUKI, Hiroyuki TAGAWA, Atsushi AOI and Koichi KAJIWARA. 2017. "Verification of Displacement Integrated from Measured Acceleration on Shake Table Experiment of Full-Scale Gymnasium Specimen". *AIJ Journal of Technology and Design.* AIJ, Vol.23, No.54, Pp:427-432. (in Japanese)

[5] Rie SUZUKI, Daiki SATO, Tomohiro SASAKI, Atsushi AOI, Koichi KAJIWARA and Hiroyuki TAGAWA. 2017. "Natural Frequency Variation and Damages in Vibration Tests of Full Scale Steel Gymnasium using E-Defense". *Journal of Structural Engineering.* AIJ, Vol.63B, Pp:241-250. (in Japanese)

[6] Daiki SATO, Hotsuki WADA, Tomohiro SASAKI, Atsushi AOI and Koichi KAJIWARA. 2018. "Evaluation of Natural Frequency and Mode Shape of Steel Gymnasium based on E-defense Shaking Table Tests". *Proc. of the 15th Japan Earthquake Engineering Symposium.* (in Japanese)